Hydrated silicate minerals on Mars observed by the Mars Reconnaissance Orbiter CRISM instrument

John F. Mustard[1], S. L. Murchie[2], S. M. Pelkey[1,2], B. L. Ehlmann[1], R. E. Milliken[3], J. A. Grant[4], J.-P. Bibring[5], F. Poulet[5], J. Bishop[6], E. Noe Dobrea[3], L. Roach[1], F. Seelos[2], R. E. Arvidson[7], S. Wiseman[7], R. Green[3], C. Hash[8], D. Humm[2], E. Malaret[8], J. A. McGovern[2], K. Seelos[2], T. Clancy[9], R. Clark[10], D. Des Marais[6], N. Izenberg[2], A. Knudson[7], Y. Langevin[5], T. Martin[3], P. McGuire[7], R. Morris[11], M. Robinson[12], T. Roush[6], M. Smith[13], G. Swayze[9], H. Taylor[2], T. Titus[14] & M. Wolff[9]

Phyllosilicates, a class of hydrous mineral first definitively identified on Mars by the OMEGA (Observatoire pour la Mineralogie, L'Eau, les Glaces et l'Activitié) instrument[1,2], preserve a record of the interaction of water with rocks on Mars. Global mapping showed that phyllosilicates are widespread but are apparently restricted to ancient terrains and a relatively narrow range of mineralogy (Fe/Mg and Al smectite clays). This was interpreted to indicate that phyllosilicate formation occurred during the Noachian (the earliest geological era of Mars), and that the conditions necessary for phyllosilicate formation (moderate to high pH and high water activity[3]) were specific to surface environments during the earliest era of Mars's history[4]. Here we report results from the Compact Reconnaissance Imaging Spectrometer for Mars (CRISM)[5] of phyllosilicate-rich regions. We expand the diversity of phyllosilicate mineralogy with the identification of kaolinite, chlorite and illite or muscovite, and a new class of hydrated silicate (hydrated silica). We observe diverse Fe/Mg-OH phyllosilicates and find that smectites such as nontronite and saponite are the most common, but chlorites are also present in some locations. Stratigraphic relationships in the Nili Fossae region show olivine-rich materials overlying phyllosilicate-bearing units, indicating the cessation of aqueous alteration before emplacement of the olivine-bearing unit. Hundreds of detections of Fe/Mg phyllosilicate in rims, ejecta and central peaks of craters in the southern highland Noachian cratered terrain indicate excavation of altered crust from depth. We also find phyllosilicate in sedimentary deposits clearly laid by water. These results point to a rich diversity of Noachian environments conducive to habitability.

High-spatial-resolution, precision-pointing and nested observations of CRISM[5], the Context Imager (CTX)[6], and the High Resolution Imaging Science Experiment (HiRISE)[7] instruments on the Mars Reconnaissance Orbiter (MRO) resolve mineralogical, stratigraphic and geological relationships for phyllosilicate deposits. This combination of instruments permits mineralogical mapping at 18 m per pixel with CRISM linked with metre-scale geomorphology from CTX and HiRISE. We focus here on the stratigraphic setting of phyllosilicate-bearing rocks in three regions and report the detection of phyllosilicate in sedimentary settings.

We identify two principal classes of mineral in the CRISM data on the basis of observed absorptions: Al phyllosilicates and the more common and spatially dominant Fe/Mg phyllosilicates. The increased spatial and spectral resolutions of CRISM have revealed a diversity of absorption band shapes, positions and combinations indicating variations in phyllosilicate type and composition (Fig. 1; see Methods for processing and identification details). Most spectra show a band at ~1.4 μm from the overtone of the OH stretch, a strong 1.9-μm H_2O band and absorptions near 2.28–2.30 μm (for example, spectrum 3 in Fig. 1b), which are consistent with Fe/Mg phyllosilicates having interlayer water, such as the smectite clays nontronite and saponite[8]. Other spectra in Nili Fossae have a dominant absorption near or longward of 2.34 μm, a weak band or inflection near 2.25 μm, and a weak or absent 1.9 μm absorption band (spectrum 4 in Fig. 1b). This combination of absorptions is consistent with high-Fe chlorites[9–11]. Some spectra from Mawrth Vallis show strong 1.9-μm and 2.2-μm features and a weak 1.4-μm band (spectrum 1 in Fig. 1b) diagnostic of montmorillonite, an Al-rich smectite clay, confirming previous detections[2]. K,Al phyllosilicates have also been recognized in a new location, the ejecta of a 50-km crater west of Nili Fossae. These spectra show 1.4-μm, 2.2-μm and ~2.35-μm absorptions but lack a 1.9-μm band (spectrum 6 in Fig. 1b). These absorptions are consistent with the presence of mica minerals such as illite and/or muscovite[10]. Additionally, in some small-scale outcrops a distinct doublet absorption with resolved absorptions at 2.16 and 2.2 μm, and a strong 1.4-μm band is observed (spectrum 5 in Fig. 1b). This combination of bands is diagnostic of kaolinite. Kaolinite was first observed by OMEGA in one small region of the southern highlands[12], whereas CRISM has observed kaolinite in Nili Fossae and Mawrth Vallis.

A new class of hydrated silicate has been identified (spectrum 2 in Fig. 1b), characterized by a 2.20–2.25-μm absorption that is distinct from that observed with Al-OH phyllosilicates such as montmorillonite in that the absorption is broader and centred at longer wavelengths. These regions commonly show 1.4-μm and 1.9-μm

[1]Department of Geological Sciences, Brown University, Providence, Rhode Island 02912, USA. [2]Johns Hopkins University/Applied Physics Laboratory, 11100 Johns Hopkins Road, Laurel, Maryland 20723, USA. [3]Jet Propulsion Laboratory, California Institute of Technology, Mail Stop 183-301, 4800 Oak Grove Drive, Pasadena, California 91109, USA. [4]Center for Earth and Planetary Studies, National Air and Space Museum, Smithsonian Institution, Independence Avenue at 6th Street SW, Washington, DC 20560, USA. [5]Institut d'Astrophysique Spatiale, Université Paris Sud 11, 91405 Orsay, France. [6]National Aeronautics and Space Administration, Ames Research Center, 515 N. Whisman Road, Mountain View, California 94043, USA. [7]Department of Earth and Planetary Sciences, Washington University, St Louis, Missouri 63130, USA. [8]Applied Coherent Technology, 112 Elden Street Suite K, Herndon, Virginia 22070, USA. [9]Space Science Institute, 4750 Walnut Street, Suite 205, Boulder, Colorado 80301, USA. [10]US Geological Survey, MS 964 Box 25046, Denver Federal Center, Denver, Colorado 80225, USA. [11]ARES Code KR, National Aeronautics and Space Administration, Johnson Space Center, 2101 NASA Parkway, Houston, Texas 77058, USA. [12]School of Earth and Space Exploration. Box 871404, Arizona State University, Tempe, Arizona 85287-1404, USA. [13]National Aeronautics and Space Administration, Goddard Space Flight Center, Code 693.0, Greenbelt, Maryland 20771, USA. [14]US Geological Survey, 2255 N. Gemini Drive, Flagstaff, Arizona, 86001, USA.
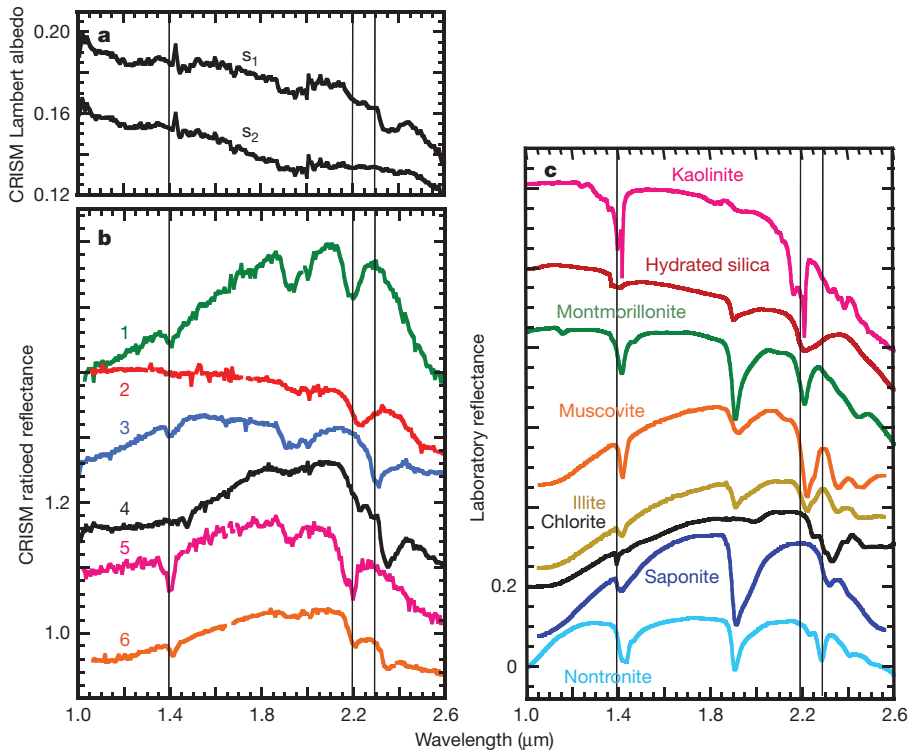
Figure 1 | CRISM and laboratory reflectance spectra showing hydrated silicate mineral diversity. **a**, CRISM reflectance spectra from 1.0 to 2.6 μm used in the spectral ratio (s_1/s_2) for spectrum 4 in **b**. **b**, Stacked spectral ratios: (1) from Mawrth Vallis, green (HRL0000285A); (2) from the southern highlands, red (FRT00035DB); (3) from Nili Fossae, blue (FRT00003E12); (4) from Nili Fossae, black (FRT00050F2); (5) from Nili Fossae, magenta (FRT00003FB9); (6) from Nili Fossae, orange (HRS0002FC5). Spectra were selected on the basis of strong BD2210 and D2300 parameter values. Vertical lines are placed at 1.4, 2.2 and 2.3 μm. **c**, Stacked library reflectance spectra of minerals with similar absorption features. The hydrated silica is an altered, hydrated volcanic ash.

bands, and this combination of spectral features is consistent with hydrated silica glasses such as opal or volcanic glass.

In the Mawrth Vallis area (Fig. 2), smectites rich in Al and Fe have been observed over a 300 km × 400 km region but are commonly found along the flanks of the outflow channel and within the surrounding plateau[13,14]. The units hosting these minerals are typically light-toned outcrops of early-Noachian to mid-Noachian materials that have been exposed by erosion from beneath a dark mantling unit that shows pyroxene absorptions. Some occurrences of phyllosilicate are clearly associated with layered rocks. This leads to
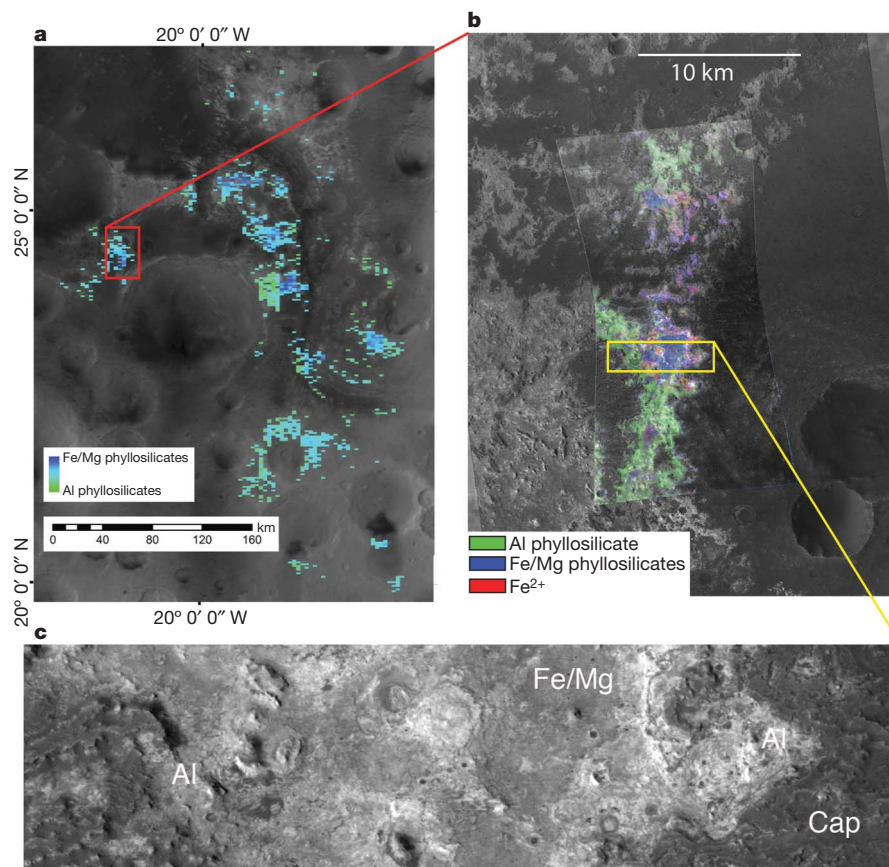
Figure 2 | Mineral diversity and stratigraphy of Mawrth Vallis. **a**, MOC map of Mawrth Vallis with OMEGA phyllosilicate mineral indicators[11] for Fe/Mg phyllosilicates (blue) and Al phyllosilicates (green). **b**, CTX image of the red box from **a**, with a superimposed mineral indicator map from CRISM observation HRL000043EC_07, in which green areas are enriched in Al phyllosilicate, blue areas are enriched in Fe/Mg phyllosilicate, and red areas indicate an Fe^{2+} slope. **c**, Subset of the CTX image from the white box in **b**, where the Fe/Mg phyllosilicate (Fe/Mg) occurs as a darker smooth surface. Al phyllosilicates (Al) are within brighter and rougher terrain beneath a capping unit (cap).

the hypothesis that they may have formed by deposition in an aqueous environment, by aqueous alteration of a volcanic ash deposit, or by impact-related alteration[13].

CRISM observation HRL000043EC falls in the region west of the mouth of Mawrth Vallis (Fig. 2a)[13]. In these light-toned outcrops we find discrete layers of Al and Fe/Mg phyllosilicates. In this region Al phyllosilicates are more prevalent (Fig. 2b); however, elsewhere in Mawrth Vallis Fe/Mg phyllosilicates are typically more abundant. In addition to CRISM spectra showing absorptions diagnostic of montmorillonite as observed previously with OMEGA, we also observe in small outcrops absorptions characteristic of kaolinite and hydrated silica or glass. Sandwiched between the Al and Fe/Mg phyllosilicate layers in CRISM image HRL000043EC is an additional material containing an Fe^{2+} slope and a broadened 2.2–2.3-µm feature.

High-resolution Mars Orbiting Camera (MOC) and High Resolution Stereo Camera (HRSC) images[13,14], as well as new observations acquired by CTX and HiRISE, reveal that the light-toned outcrops in Mawrth Vallis are layered and often show a distinct polygonal texture. The Fe/Mg-phyllosilicate-bearing unit is the lowest stratigraphic level and is overlain by Al-phyllosilicate-bearing strata; both are exposed by erosion from beneath a dark-toned capping unit (Fig. 2c). Despite the close proximity of these phyllosilicate-bearing units, we see no evidence for mixing of the two phyllosilicate signatures at spatial resolutions of ~40 m per pixel. This indicates that the minerals occur in spatially distinct stratigraphic units.

The Nili Fossae region shows expansive outcrops of phyllosilicates[2,12] but also extensive spectral signatures of olivine in close proximity[15–19]. Several high-resolution observations across this region (Fig. 3a) show that much of the olivine is present within aeolian bedforms. However, several observations provide definitive evidence for the presence of phyllosilicate-bearing units in direct contact with unaltered olivine-bearing units. In CRISM observation FRT00003E12, stratigraphic relationships are resolved between the lowest, phyllosilicate-bearing bedrock unit and the overlying olivine-bearing bedrock unit (Fig. 3b). The phyllosilicate-rich unit shows polygonal fractures and is recessed on slope-forming units, suggesting that it is more easily eroded than the cap unit. The phyllosilicate unit is capped by a regionally extensive, spectrally neutral, mesa-forming unit. Although most of the cap unit is massive, HiRISE data show the base is tens of metres thick and contains banding and/or layering (Fig. 3c). Coordinated CRISM data show this banded unit is olivine-rich and that it rests directly on top of the phyllosilicate-rich material (Fig. 3c). This sequence of a spectrally neutral cap rock overlying an unaltered olivine-rich unit resting on phyllosilicate-rich rocks is observed in CRISM observations across a distance of 2,000 km from the Nili Fossae region to the southern edge of the Isidis Basin[20].

CRISM has targeted contacts between phyllosilicate-bearing rocks and Hesperian-aged lavas from Syrtis Major. Some of the observations are of high-standing Noachian-aged massifs embayed by lava (FRT000050F2 and FRT00005A3E) and other observations show phyllosilicate-bearing outcrops beneath volcanic plains (FRT000048B2, and Fig. 3d). In all these observations of volcanic rocks in contact with phyllosilicate-bearing terrains, the volcanic rocks are unaltered and provide no evidence for hydrated silicates. A section of the Nili Fossae trough scarp that is ~600 m high exposes rocks that are strongly enriched in phyllosilicates, whereas the rocks capping the plateau are enriched in pyroxene (Fig. 3d).

In the ancient southern highlands, localized phyllosilicate deposits were identified with OMEGA data[19,21]. With the use of a combination of multispectral mapping and targeted observations, CRISM has significantly expanded the number of locations to the thousands of phyllosilicate occurrences (see, for example, Fig. 4a). These data show phyllosilicates associated with craters of many sizes and within ejecta, walls and central peaks. Full-resolution CRISM observation FRT000049BB shows a highlands crater in which Fe/Mg smectite clays are can be seen in outcrops at or near the rim of the crater along

its inward facing wall (Fig. 4b). Weaker phyllosilicate detections are visible downslope of these outcrops, indicating physical breakdown and mass wasting. In addition we observe phyllosilicate associated with ejecta exterior to the crater and in mounds and knobs on the crater floor. CRISM observation FRT00003E92 shows Fe/Mg phyllosilicates associated with the central peak of a crater 45 km in diameter (Fig. 4c). This central peak material probably originated from a depth of 4–5 km, indicating alteration of the crust to at least this depth. Elsewhere in the southern highlands we observe phyllosilicates in central peaks that show a distinct 2.2-µm absorption indicative of either Al phyllosilicate or hydrated glass (Fig. 1).
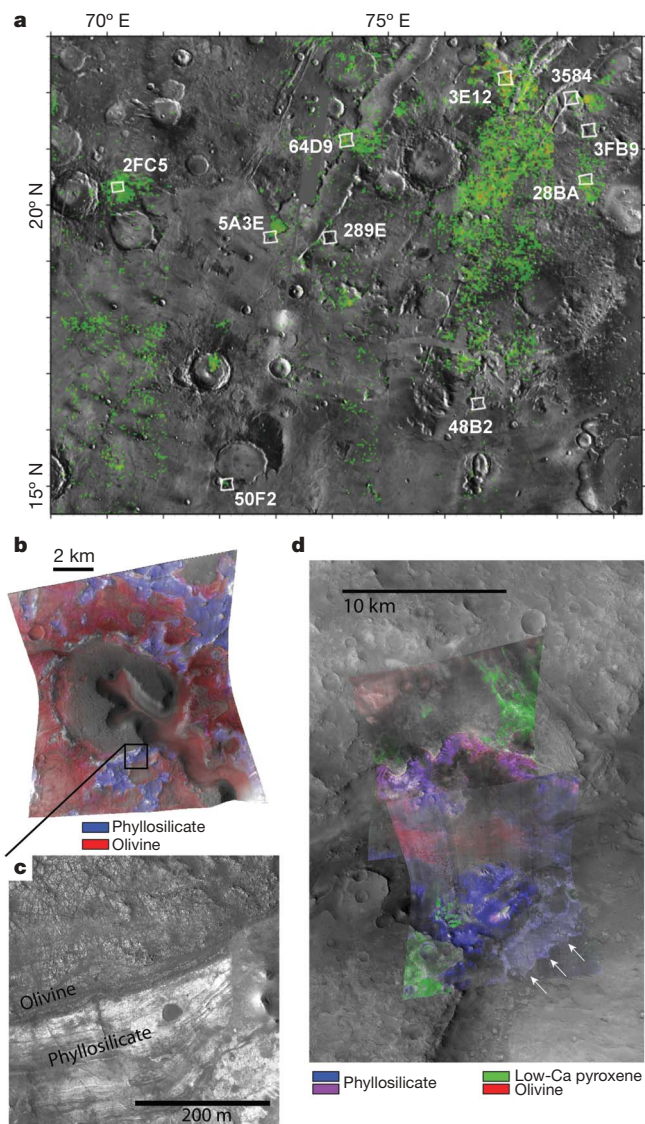
Figure 3 | Stratigraphy of phyllosilicate-bearing strata in the Nili Fossae region. a, OMEGA phyllosilicate detections (green) based on the D2300 parameter[11] overlaid on a Viking digital image mosaic. Targeted CRISM images are outlined; their full identifications are preceded by FRT0000. **b**, CRISM scene FRT00003E12 overlaid with CRISM mineral indicators of olivine (red) and phyllosilicate (blue). The black box indicates the location of **c**. **c**, A portion of HiRISE image PSP_002176_2025. Phyllosilicates are found in the bright layered material, overlain by a thin (one or two CRISM pixels) layer of olivine capped by a spectrally neutral unit. **d**, Mineral indicators from CRISM observations FRT000064D9 and FRT00007BC8 overlaid on CTX observation P05_003986_20_11_XI_21N285W_070324. Low-Ca pyroxene is shown in green, phyllosilicate in blue and magenta, and olivine in red. The boundary between Syrtis Major lava and phyllosilicate-bearing material within Nili Fossae trough material is shown by the white arrows.

Phyllosilicates have also been identified by CRISM within sedimentary basins, specifically in fans and deltas within Holden, Eberswalde and Jezero craters, and represent the detection on Mars of hydrated silicates within sediments clearly deposited by water. The mineralogy of phyllosilicates within the sedimentary deposits does not differ from that in nearby potential sediment source regions, whether interior to the basin, as in Holden[22,23], or from Jezero crater's exterior catchment[24]. The sedimentary phyllosilicates may have been eroded and transported rather than being formed *in situ*, although formation *in situ* cannot be ruled out; it is likely that some alteration of materials within the crater occurred during the various periods of aqueous activity. However, there is a relative paucity of phyllosilicate spectral signatures in the uppermost units of the sedimentary deposits, implying that conditions favouring phyllosilicate formation, deposition or preservation did not persist into the late stages of delta formation in the Noachian.

The CRISM observations and coordinated CTX and HiRISE imaging showed detailed geological relationships and compositional stratigraphy. In the Nili Fossae and Isidis regions we observe regionally extensive phyllosilicate-bearing rocks overlain by both unaltered rocks susceptible to alteration (olivine, pyroxene) and/or a spectrally neutral mesa-forming unit and embayed by Hesperian Syrtis Major

lavas that show no evidence of alteration. Some of the rock units in this region are cut by fractures associated with the Isidis impact basin, which is dated to the late Noachian. Because the olivine-bearing units were emplaced before or concurrently with the event that formed the Isidis basin[17,19], the lack of any aqueous alteration associated with the olivine lithologies, and the lack of alteration of Hesperian lavas, definitively document Noachian phyllosilicate formation.

The Mawrth Vallis and Nili Fossae regions show that thick, regionally extensive sections of Noachian crust are altered. Throughout the southern highlands, CRISM data document phyllosilicates in the walls, ejecta and central peaks of craters in the southern highlands. This striking association of phyllosilicates with impact craters may be the result of impacts excavating pre-existing deposits or impact-associated processes, leading to the formation of phyllosilicate and hydrated silicate minerals. The possibility cannot be excluded that the alteration occurred as a result of the impact hydrothermal processes[25,26]. However, these systems are usually restricted to the subsurface and/or interior of craters (for example melt sheets). The uniform distribution of phyllosilicate-rich material in crater ejecta, and the presence of phyllosilicates in the walls, floor deposits and within central peaks, argue for the presence of hydrated silicates in the target rocks before impact. With hydrated silicates observed in central peaks of impact
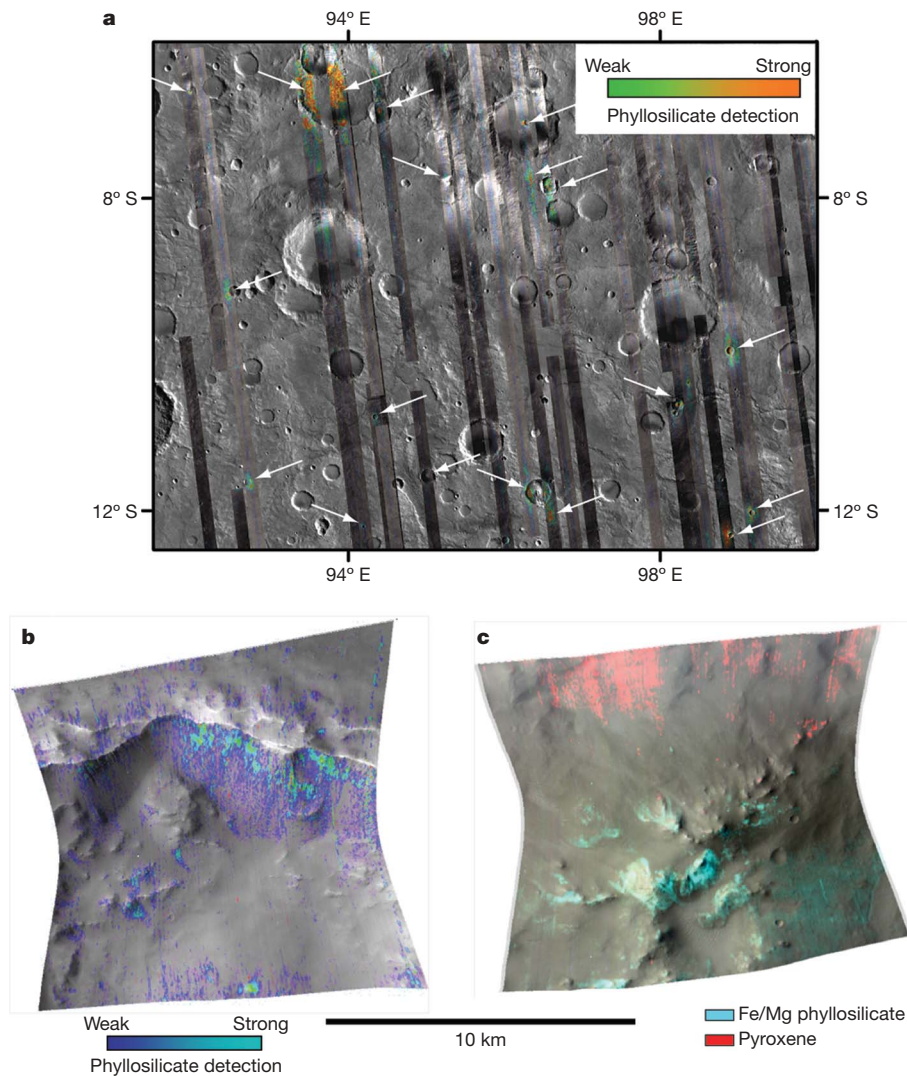
Figure 4 | Phyllosilicate occurrences in the Noachian-aged southern highlands. a, Map of phyllosilicate mineral indicator[11] (green, weak; orange, strong) derived from CRISM multispectral mapping merged with a MOC wide-angle camera image mosaic. White arrows show distinct regions enriched in phyllosilicate. **b**, High-resolution CRISM observation FRT000049BB at 13.25° S, 105.25° E, showing a phyllosilicate mineral indicator map (blue, low; green, high). **c**, High-resolution CRISM observation FRT00003E92 at 13.5° S, 119.5° E, showing phyllosilicate (cyan) and pyroxene (red) mineral indicator maps.

craters on the order of 45 km, a significant thickness of the ancient martian crust has experienced some form of alteration. In contrast, despite many observations, no craters in terrains of Hesperian age or in the northern plains where subsurface ice is known to be present show evidence for phyllosilicates.

Identifying the types of phyllosilicate minerals on Mars also constrains their environment of formation. The majority of phyllosilicate spectra are most consistent with smectite clay minerals such as montmorillonite, nontronite and saponite. Smectite clays require significant water reservoirs and moderate to alkaline pH (ref. 3). However, the higher spatial resolution of CRISM has augmented the phyllosilicate mineral diversity beyond this class alone. CRISM has expanded the geographic range of Al–OH-bearing phyllosilicates with a new detection in the Nili Fossae region, where spectra are more consistent with illite or muscovite and kaolinite rather than with montmorillonite. In addition, several regions show absorption features consistent with chlorite. Overall, the weathering products of Fe/Mg mafic minerals are over-represented relative to alkaline minerals such as plagioclase, given the basaltic mineralogy of the martian crust. Kaolinite, which would be expected from an active hydrological system operating in regions with good drainage and high levels of flushing[27], has been identified in only a few locations, and exposures are less than 200 m × 200 m in spatial scale. The restriction of kaolinite to such rare, small deposits argues against a widespread and vigorous hydrological system in the Noachian or the possibility that the lifetime of such a system was sufficient for the formation of smectite clay but not kaolinite. However, the existence of localities with kaolinite and other diverse phases such as chlorite and hydrated silica suggests that microenvironments with a greater throughput of liquid water or enhanced hydrothermal activity were also a feature of early Mars.

METHODS SUMMARY

Standard processing approaches were used to convert CRISM data from instrument units to apparent I/F (the ratio of reflected intensity to incident intensity of sunlight) (ref. 5). We then assume a lambertian surface and divide the data by the cosine of the incidence angle. We assume that surface and atmospheric contributions are multiplicative and that the atmospheric contribution follows an exponential variation with altitude[28]. The data are divided by a scaled, atmospheric transmission spectrum obtained from an observation across Olympus Mons, as used by the OMEGA instrument team[1,15]. This method removes only the effects of gas absorption. However, it is efficient for the analysis of large volumes of data and compares favourably with a more rigorous but time-intensive retrieval of surface Lambert albedos using DISORT-based simulations and regressions for each wavelength band between modelled CRISM radiances and a suite of input surface albedos[29] that addresses both gas absorptions and aerosols. Spectral summary parameters are then derived for each observation, to highlight areas with interesting mineralogy[30].

Narrow absorptions in the 1.9–2.5-µm wavelength region are due to combinations of molecular vibrations in phyllosilicate minerals. Residual calibration artefacts and errors in atmospheric removal cause systematic spikes (Fig. 1a) that are suppressed in spectral ratios in which the spectrum for a region of interest is divided by the spectrum of a nearby region of low spectral contrast. If water is present in a mineral (for example interlayer water in smectite clays), then an absorption centred near 1.9 µm is observed as a result of the combination of the H–O–H bending and stretching vibrations[29]. Absorptions near 2.2 µm are indicative of Al–OH vibrations, whereas those between 2.28 and 2.35 µm are commonly indicative of Fe/Mg–OH vibrations[8–10]. Quantitative abundances can be estimated from computationally intensive, nonlinear spectral deconvolution[31]. Thus, our analyses focus on the detection of phyllosilicate mineralogy, and a qualitative measure of relative abundance is provided by the spectral parameters[30].

1. Bibring, J. P. et al. Mars surface diversity as revealed by the OMEGA/Mars Express observations. *Science* 307, 1576–1581 (2005).
2. Poulet, F. et al. Phyllosilicates on Mars and implications for early martian climate. *Nature* 438, 623–627 (2005).
3. Velde, B., Righi, D., Meunier, A., Hillier, S. & Inoue, A. in *Origin and Mineralogy of Clays* (ed. Velde, B.) 8–42 (Springer, Berlin, 1995).
4. Bibring, J. P. et al. Global mineralogical and aqueous Mars history derived from OMEGA/Mars Express data. *Science* 312, 400–404 (2006).
5. Murchie, S. et al. Compact Reconnaissance Imaging Spectrometer for Mars (CRISM) on Mars Reconnaissance Orbiter (MRO). *J. Geophys. Res.* 112, doi:10.1029/2006JE002682 (2007).
6. Malin, M. C. et al. Context Camera Investigation on board the Mars Reconnaissance Orbiter. *J. Geophys. Res.* 112, E05S04, doi:10.1029/2006JE002808 (2007).
7. McEwen, A. S. et al. Mars Reconnaissance Orbiter's High Resolution Imaging Science Experiment (HiRISE). *J. Geophys. Res.* 112, E05S02, doi:10.1029/2005JE002605 (2007).
8. Frost, R. L., Kloprogge, J. T. & Ding, Z. Near-infrared spectroscopic study of nontronites and ferruginous smectite. *Spectrochim. Acta A Mol. Biomol. Spectrosc.* 58, 1657–1668 (2002).
9. Bishop, J., Madejova, J., Komadel, P. & Froschl, H. The influence of structural Fe, Al and Mg on the infrared OH bands in spectra of dioctahedral smectites. *Clay Miner.* 37, 607–616 (2002).
10. Clark, R. N., King, T. V. V., Klejwa, M., Swayze, G. A. & Vergo, N. High spectral resolution reflectance spectroscopy of minerals. *J. Geophys. Res. Solid Earth Planets* 95, 12653–12680 (1990).
11. Calvin, W. M. Could Mars be dark and altered? *Geophys. Res. Lett.* 25, 1597–1600 (1998).
12. Poulet, F. et al. Discovery, mapping and mineralogy of phyllosilicates on Mars by MEx-OMEGA: A reappraisal. *Seventh International Conference on Mars*. abstract 3170 (2007).
13. Loizeau, D. et al. Phyllosilicates in the Mawrth Vallis region of Mars. *J. Geophys. Res.* 112, E08S08, doi:10.1029/2006JE002877 (2007).
14. Michalski, J. R. & Dobrea, E. Z. N. Evidence for a sedimentary origin of clay minerals in the Mawrth Vallis region, Mars. *Geology* 35, 951–954 (2007).
15. Mustard, J. F. et al. Olivine and pyroxene diversity in the crust of Mars. *Science* 307, 1594–1597 (2005).
16. Hoefen, T. M. et al. Discovery of olivine in the Nili Fossae region of Mars. *Science* 302, 627–630 (2003).
17. Hamilton, V. E. & Christensen, P. R. Evidence for extensive, olivine-rich bedrock on Mars. *Geology* 33, 433–436 (2005).
18. Mustard, J. F. et al. Mineralogy of the Nili Fossae region with OMEGA/Mars Express data: 1. Ancient impact melt in the Isidis Basin and implications for the transition from the Noachian to Hesperian. *J. Geophys. Res.* 112, E08S03, doi:10.1029/2006JE002834 (2007).
19. Mangold, N. et al. Mineralogy of the Nili Fossae region with OMEGA/Mars Express data: 2. Aqueous alteration of the crust. *J. Geophys. Res.* 112, E08S04, doi:10.1029/2006JE002835 (2007).
20. Bishop, J. L. et al. Characterization of phyllosilicates in Libya Montes and the southern Isidis Planitia region using CRISM and HiRISE images. *Seventh International Conference on Mars* (Pasadena, California, abstract 3294 (2007).
21. Costard, F. et al. Detection of hydrated minerals on fluidized ejecta lobes from OMEGA observations: implications in the history of Mars. *37th Lunar and Planetary Science Conference, Houston, Texas* abstract 1288 (2006).
22. Grant, J. A. et al. HiRISE imaging of impact megabreccia and sub-meter aqueous strata in Holden crater, Mars. *Geology* 36, 195–198 (2008).
23. Milliken, R. E. et al. Clay minerals in Holden crater as observed by MRO CRISM. *7th International Mars Conference*. abstract 3282 (2007).
24. Ehlmann, B. L. et al. Clay minerals in delta deposits and organic preservation potential on Mars. *Nature Geosci..* doi:10.1038/ngeo207 (2008).
25. Newsom, H. E. Hydrothermal alteration of impact melt sheets with implications for Mars. *Icarus* 44, 207–216 (1980).
26. Rathbun, J. A. & Squyresb, S. W. Hydrothermal systems associated with Martian impact craters. *Icarus* 157, 362–372 (2002).
27. Srodon, J. Nature of mixed-layer clays and mechanisms of their formation and alteration. *Annu. Rev. Earth Planet. Sci.* 27, 19–53 (1999).
28. Bibring, J. P. et al. Results from the ISM Experiment. *Nature* 341, 591–593 (1989).
29. Wolff, M. J. Constraints on dust aerosols from the Mars Exploration Rovers using MGS overflights and Mini-TES. *J. Geophys. Res.* 111, E12S17, doi:10.1029/2006JE002786 (2006).
30. Pelkey, S. M. et al. CRISM multispectral summary products: Parameterizing mineral diversity on Mars from reflectance. *J. Geophys. Res.* 112, E08S14, doi:10.1029/2006JE002831 (2007).
31. Poulet, F. & Erard, S. Nonlinear spectral mixing: Quantitative analysis of laboratory mineral mixtures. *J. Geophys. Res.* 109, E02009, doi:10.1029/2003JE002179 (2004).